Chinese Chemical Letters 36 (2025) 110205

Contents lists available at ScienceDirect

Chinese Chemical Letters

journal homepage: www.elsevier.com/locate/cclet

Adsorption and visual detection of nitro explosives by pillar[*n*]arenes-based host–guest interactions

Xueru Zhao[a], Aopu Wang[a], Shimin Wang[a], Zhijie Song[a], Li Ma[c], Li Shao[a,b,*]

[a] Department of Materials Science and Engineering, Zhejiang Sci-Tech University, Hangzhou 310018, China
[b] Zhejiang Provincial Innovation Center of Advanced Textile Technology, Shaoxing 312000, China
[c] Department of Chemistry, University of Missouri, Columbia, Missouri 65211, United States

ARTICLE INFO

Article history:
Received 29 February 2024
Revised 26 June 2024
Accepted 2 July 2024
Available online 2 July 2024

Keywords:
Pillar[*n*]arenes
Host–guest interactions
Aromatic nitro compounds
Adsorptive separation
Explosive detection

ABSTRACT

Aromatic nitro compounds present substantial health and environmental concerns due to their toxic nature and potential explosive properties. Consequently, the development of host–guest molecular recognition systems for these compounds serves a dual-purpose: enabling the fabrication of high-performance sensors for detection and guiding the design of efficient adsorbents for environmental remediation. This study investigated the host–guest recognition behavior of perethylated pillar[*n*]arenes toward two aromatic nitro molecules, 1-chloro-2,4-dinitrobenzene and picric acid. Various techniques including ^{1}H NMR, 2D NOESY NMR, and UV-vis spectroscopy were employed to explore the binding behavior between pillararenes and aromatic nitro guests in solution. Moreover, valuable single crystal structures were obtained to elucidate the distinct solid-state assembly behaviors of these guests with different pillararenes. The assembled solid-state supramolecular structures observed encompassed a 1:1 host–guest inclusion complex, an external binding complex, and an exo-wall tessellation complex. Furthermore, based on the findings from these systems, a pillararene-based test paper was developed for efficient picric acid detection, and the removal of picric acid from solution was also achieved using pillararenes powder. This research provides novel insights into the development of diverse host–guest systems toward hazardous compounds, offering potential applications in environmental protection and explosive detection domains.

Aromatic nitro compounds refer to compounds in which one or more nitro groups ($-NO_2$) are present on an aromatic ring. These compounds hold great significance in various chemical industries, including explosives [1,2], dyes [3], pharmaceuticals [4], and other fields [5]. However, their production and utilization can lead to environmental pollution, with a particular concern in the explosives industry [6,7]. Of all the aromatic nitro explosives, picric acid, also known as 2,4,6-trinitrophenol, is highly explosive with a high detonation velocity, consequently used in the explosives and firework industry [8]. As a result, picric acid has become a major environmental pollutant. And the release of picric acid into the environment from industrial sources has posed a significant risk of accidental explosions, attributed to its inherent instability and sensitivity when triggered by decomposition or aging processes [9]. Besides, nitro compounds are highly toxic and can cause severe burns and skin irritation upon contact [10]. Consequently, it is of great significance to explore novel materials and methods for the effective detection and adsorption of aromatic nitro compounds to address these concerns.

In recent years, macrocycles-based host–guest molecular recognition system has attracted significant attention due to their wide application in sensor [11-13], biotechnology [14,15], adsorption and separation [16-19]. Host–guest molecular recognition exhibits high selectivity and specificity [20-22]. The host molecule recognizes and binds to the guest molecule based on complementary features [23-27]. We hypothesized that the utilization of the macrocyclic host could recognize and adsorb nitro explosives through host–guest interactions. Considering the electron-deficiency nature of nitro explosives, herein we chose the pillar[*n*]arenes containing electron-rich aromatic wall serving as hosts [28]. This study presented the discovery of the complexation between perethylated pillar[*n*]arenes and two aromatic nitro compounds: 1-chloro-2,4-dinitrobenzene (**G1**) and picric acid (**G2**). The host–guest complexation modes in solution and solid state were both investigated in detail. Additionally, pillar[*n*]arenes powders exhibited detection and adsorption ability for nitro compounds, offering a novel strategy for mitigating environmental hazards.

* Corresponding author.
E-mail address: lishao@zstu.edu.cn (L. Shao).

https://doi.org/10.1016/j.cclet.2024.110205
1001-8417/

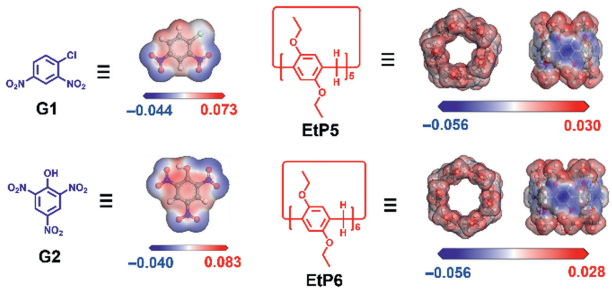

Scheme 1. Chemical structures and electrostatic potential maps of **G1**, **G2**, **EtP5** and **EtP6**.

We initiated our study by computing the electrostatic potential maps of pillar[*n*]arenes, which uncovered the electron-rich nature of their aromatic walls (indicated by the blue area, suggesting an abundance of electrons, as illustrated in Scheme 1). Furthermore, we assessed the electron distribution of **G1** and **G2** by calculating their respective electrostatic potential maps. Interestingly, both **G1** and **G2** exhibited a significant electron deficiency in their aromatic regions (indicated by the red area, suggesting a relative absence of electrons). Based on these findings, we proposed that pillar[*n*]arenes, including perethylated pillar[5]arenes (**EtP5**) and pillar[6]arenes (**EtP6**) may possess a strong binding capability towards electron-poor nitro compounds through charge-transfer interactions, owing to their electronic complementarity.

Subsequently, we investigated the host–guest interactions between pillar[*n*]arenes and the nitro compounds in solution using NMR techniques. Upon introducing **EtP5** into the **G1** solution, no noticeable chemical shifts of the proton signals were observed on **G1**, indicating a lack of complexation behavior between **EtP5** and **G1** (Figs. S1a–c in Supporting information). This could be attributed to the relatively small cavity size of **EtP5**, which makes it challenging to accommodate the **G1** guest. In contrast, the NMR spectrum of the **EtP6** and **G1** mixture exhibited chemical shifts (Figs. S2a–c in Supporting information). The addition of **EtP6** induced upfield shifts in all proton signals of **G1** ($\Delta\delta = -0.036$, –0.054, and –0.062 ppm for H_{1a}, H_{1b}, and H_{1c}, respectively), attributed to the shielding effect of the protons (Figs. S2a–c). Additionally, nuclear overhauser effect (NOE) correlations were observed between protons H_{1a}, H_{1b}, and H_{1c} on **G1** and protons $H_{2'}$ and $H_{3'}$ on **EtP6**, providing evidence for the encapsulation of **G1** within the cavity of **EtP6**, forming an inclusion complex (Fig. S2d in Supporting information).

Upon addition of **EtP5** and **EtP6** to **G2**, upfield shifts were observed in the proton signal H_{2a} of **G2** ($\Delta\delta = -0.028$ and –0.026 ppm, for complexing with **EtP5** and **EtP6**, respectively, Figs. 1a–c and Figs. S3a–c in Supporting information). To understand the relative spatial positions within the host–guest inclusion complexes, the 2D NOESY NMR experiments were conducted. NOE signals were also found between H_{2a} on **G2** and $H_{1\text{-}4}$, $H_{1'\text{-}4'}$ on **EtP5** and **EtP6**, respectively, indicating these protons were in close proximity to each other (Fig. 1d and Fig. S3d in Supporting information).

Notably, upon dissolving these host–guest complexes of **EtP6** and **G1**, **EtP5** and **G2**, **EtP6** and **G2** in chloroform, the color of the solution underwent a significant change, which differed from the clear solution of the individual host and guest (inset picture in Figs. 2a–d). The host–guest complex of **EtP5** and **G1** showed a slight color change, which might be attributed to the weak host–guest interactions. The UV-vis spectra of the host–guest complexes revealed a broad absorption band at 420 nm, indicating characteristic absorption resulting from charge transfer interactions within the host–guest complexes (Figs. 2a–d). To determine the binding affinity of the host–guest complexes, fluorescent titration experiments

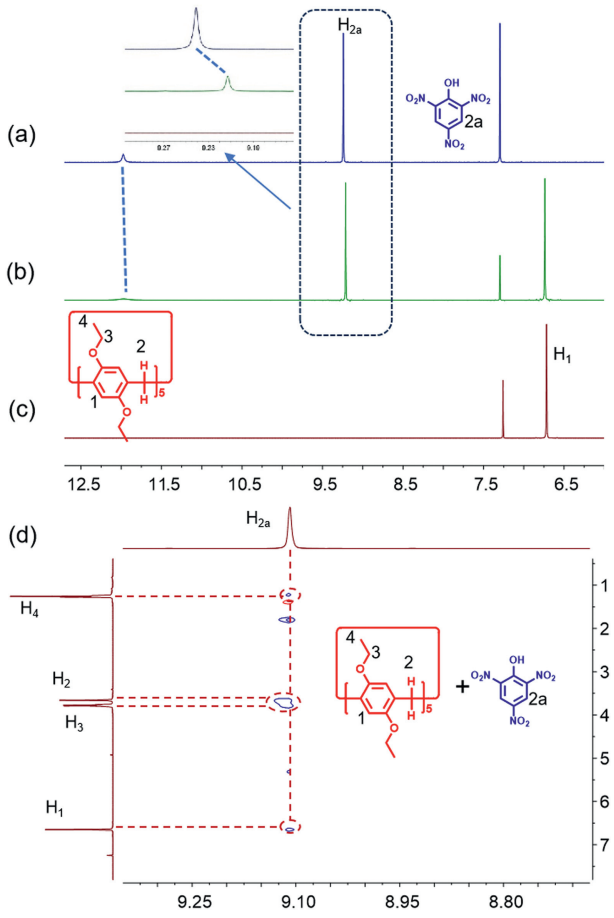

Fig. 1. Partial ^{1}H NMR spectra (400 MHz, $CDCl_3$, 293 K): (a) **G2**, (b) a mixture of **G2** (10.0 mmol/L) and **EtP5** (10.0 mmol/L) and (c) **EtP5**. (d) Partial NOESY NMR spectrum (500 MHz, $CDCl_3$, 293 K): **G2** (10.0 mmol/L) and **EtP5** (10.0 mmol/L).

were conducted (Figs. S4–S13 in Supporting information). The fluorescence was significantly quenched upon adding guest to the host solution. Based on the fluorescent titration results, molar ratio plot and non-linear curve fitting were utilized to obtain the stoichiometry and association constant of these host–guest complexes. The stoichiometry of **EtP5** and **G2** were calculated to be 1:2, with association constants determined to be $(5.90 \pm 1.35) \times 10^3$ and $(1.48 \pm 0.30) \times 10^4$ L/mol for K_1 and K_2, respectively (Figs. S7–S10). The cooperativity factor α ($\alpha = 4K_2/K_1$) were calculated to be 7.01 ($\alpha > 1$), suggesting a positive cooperativity. The binding constant of the complex of **EtP6** and **G2** was calculated to be $(9.63 \pm 2.57) \times 10^4$ L/mol with a 1:1 stoichiometry, higher than that of **EtP5** and **G2** (Figs. S11–S13). This finding suggested that **EtP6** might provide a deeper cavity for the guest molecules, leading to an increased binding affinity towards **G2**. The association constant of the complex of **EtP6** and **G1** was calculated to be $(1.76 \pm 0.26) \times 10^4$ L/mol, lower than that of **EtP6** and **G2** (Figs. S4–S6). This indicated that an increase in nitro groups on the guest might enhance intermolecular charge-transfer interactions, resulting in a stronger binding affinity.

Other than investigating the host–guest interaction in solution, single crystals were cultivated to investigate the solid-state assembly behavior between pillararenes and these nitro-compounds. Single crystals of **EtP6⊃G1** were obtained through the gradual evaporation of a mixed solution containing chloroform and ethanol. Analysis using X-ray crystallography revealed that **EtP6⊃G1** crystallized in the monoclinic *C*2/*c* space group, with one molecule of **EtP6** and one molecule of **G1** present in each unit cell. The crys-

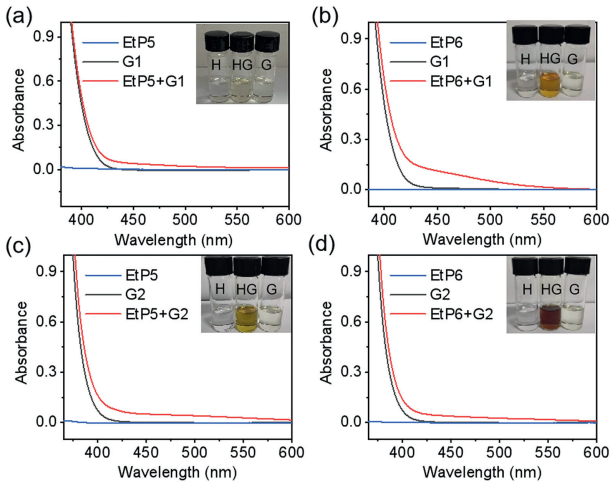

Fig. 2. UV-vis spectra ($CHCl_3$) of (a) (**H**) **EtP5** (5.0 mmol/L), (**G**) **G1** (20.0 mmol/L), (**HG**) **EtP5** (5.0 mmol/L) and **G1** (20.0 mmol/L); (b) (**H**) **EtP6** (5.0 mmol/L), (**G**) **G1** (20.0 mmol/L), (**HG**) **EtP6** (5.0 mmol/L) and **G1** (20.0 mmol/L); (c) (**H**) **EtP5** (5.0 mmol/L), (**G**) **G2** (20.0 mmol/L), (**HG**) **EtP5** (5.0 mmol/L) and **G2** (20.0 mmol/L); and (d) (**H**) **EtP6** (5.0 mmol/L), (**G**) **G2** (20.0 mmol/L), (**HG**) **EtP6** (5.0 mmol/L) and **G2** (20.0 mmol/L).

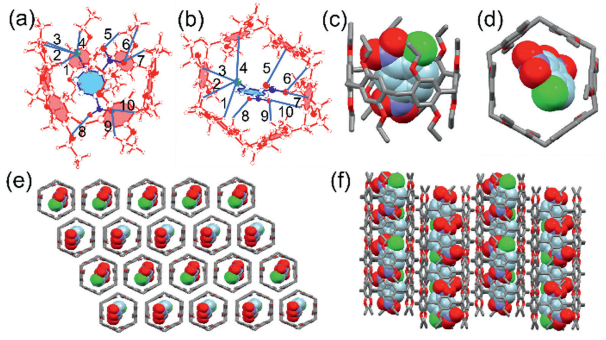

Fig. 3. (a, b) Ball-stick views of the crystal structures of **EtP6⊃G1**. Host **EtP6** is red, guest **G1** is blue, oxygen atoms are solid and red, and nitrogen atoms are solid and blue. In **EtP6⊃G1**, **1**–**4** indicating C–H···Cl interactions, **5**–**10** indicating C–H···O interactions. (c, d) Crystal structure of the host–guest complex between **EtP6** and **G1**. Host **EtP6** is in a capped stick model, and guest **G1** is in a space-filling model. (e, f) Packing structure of **EtP6⊃G1**, revealing that the guest molecules were encapsulated in the one-dimensional channel formed by **EtP6**.

tal structure clearly demonstrated the formation of a 1:1 host–guest inclusion complex between **G1** and **EtP6**. Notably, in the **EtP6⊃G1** complex, each **G1** molecule was fully encapsulated by an **EtP6** molecule, and various hydrogen bonding interactions could be observed. The main driving forces behind these interactions were C–H···Cl and C–H···O interactions (**1**–**10** in Figs. 3a and b). Specifically, the chlorine atom on **G1** interacted with four hydrogen atoms from the ethoxy group on **EtP6** at calculated distances of 3.11, 3.18, 3.02, and 3.63 Å (**1**–**4**), respectively. Additionally, C–H···O interactions (**5**–**10**) were observed between the oxygen atoms of the nitro group on **G1** and the hydrogen atoms of the ethoxy group on **EtP6**. All of these noncovalent interactions collectively contributed to stabilizing the threading structure of **EtP6⊃G1** in the solid state (Figs. 3c and d). From the extending structure of the host–guest complex, **G1** molecules were found to locate inside the one-dimensional channel formed by **EtP6**, indicating a good encapsulation ability for **EtP6** toward **G1** (Figs. 3e and f).

The single crystals of **EtP5@G2** were obtained through the gradual evaporation of a mixed solution containing chloroform and hexane. The crystal structure of **EtP5@G2** exhibited a monoclinic *C*2/*c* space group, with an exo-wall binding mode. This host–guest

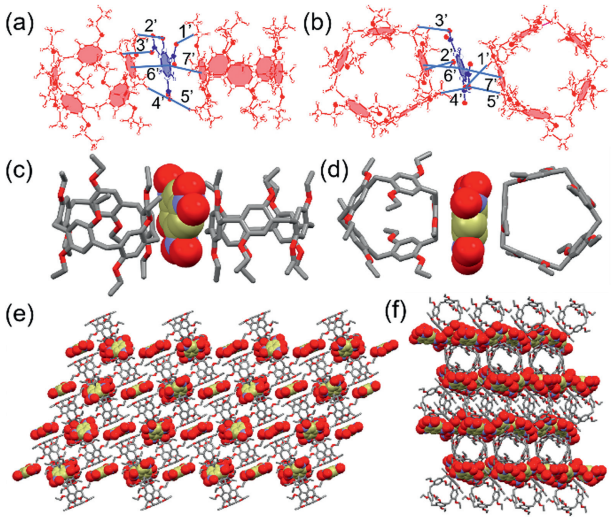

Fig. 4. (a, b) Ball-stick views of the crystal structures of **EtP5@G2**. Host **EtP5** is red, guest **G2** is blue, oxygen atoms are solid and red, and nitrogen atoms are solid and blue. In **EtP5@G2**, **1'**–**5'** indicate C–H···O interactions, **6'** and **7'** indicate π–π interactions. (c, d) Crystal structure of the host–guest complex between **EtP5** and **G2**. Host **EtP5** is in a capped stick model, and guest **G2** is in a space-filling model. (e, f) Packing structure of **EtP5@G2**, revealing that the guest molecules formed external binding complex with host molecules.

complex was stabilized by multiple hydrogen bonding and π–π stacking interactions (Figs. 4a and b). Specifically, five C–H···O interactions (**1'**–**5'**) were observed between the oxygen atoms of the nitro and phenol groups on **G2** and the hydrogen atoms on **EtP5**. The H···O distances measured were 2.70, 2.79, 2.96, 2.85, and 2.85 Å (**1'**–**5'**, respectively). Furthermore, π–π interactions were identified between the ring plane of **G2** and the adjacent ring plane of **EtP5**. The distances between the aromatic centroid of **G2** and the ring plane of **EtP5** were measured as 3.25 and 3.35 Å (**6'** and **7'**, respectively). Analysis of the crystal packing revealed that **G2** resided within the gap between **EtP5** molecules, with each **G2** molecule sandwiched by two **EtP5** molecules through exo-wall charge transfer interactions (Figs. 4c–f).

The host–guest complex between **EtP6** and **G2** in solid state was also investigated. The **EtP6@G2** complex crystallized from a mixed solution of chloroform and hexane. The crystal structure has an orthorhombic $Pna2_1$ space group, with one molecule of **EtP6** and four molecules of **G2** present per unit cell. **G2** was also associated with **EtP6** *via* exo-wall interactions. As revealed from the crystal structure, eight hydrogen bonds and two π–π stacking interactions were found between **EtP6** and **G2** (Figs. 5a and b). The H···O distance of these hydrogen bonds was measured to be 2.68, 2.87, 2.82, 2.94, 2.95, 2.93, 2.79, and 2.85 Å (**1"**–**8"**, respectively). Moreover, for the π–π stacking interactions, the distance between centroid of the aromatic ring on **G2** and the ring plane on **EtP6** was measured to be 3.25 and 3.35 Å (**9"** and **10"**, respectively). **G2** also interacted with adjacent **EtP6** molecules, through parallel face-to-face π–π stacking with benzene faces of **EtP6** (Figs. 5c and d). In the packing structure, each side of **EtP6** was found to be surrounded by **G2**, resulting in the formation of the two-dimensional tessellation (Figs. 5e and f). From the crystal structure it was found that **EtP6** held a strong host–guest binding ability toward **G2** in solid state.

Furthermore, we investigated the potential development of a sensor system for the detection of nitro-compounds based on these host–guest systems. Each guest (**G1**, **G2**) was dissolved in methanol solution with a concentration of 0.2 mol/L, and then pillararenes powders were suspended into the solution to allow for solid-liquid adsorption. Pillararenes powders were then cen-

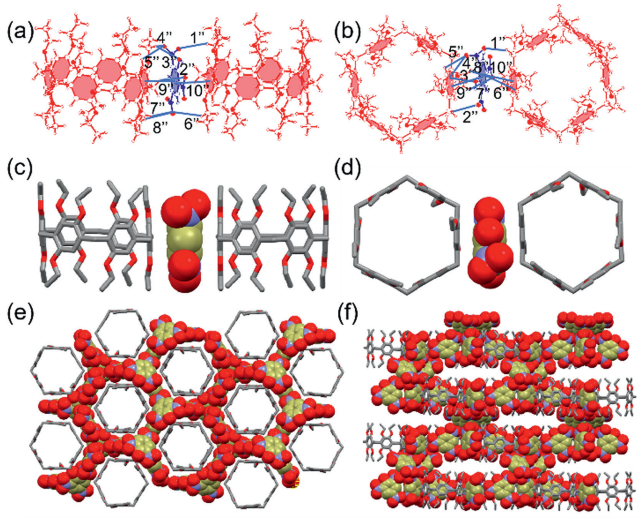

Fig. 5. (a, b) Ball-stick views of the crystal structures of **EtP6⊃G2**. Host **EtP6** is red, guest **G2** is blue, oxygen atoms are solid and red, and nitrogen atoms are solid and blue. In **EtP6⊃G2**, **1'–8'** indicate C–H···O interactions, **9'** and **10'** indicate π–π interactions. (c, d) Crystal structure of the host-guest complex between **EtP6** and **G2**. Host **EtP6** is in a capped stick model, and guest **G2** is in a space-filling model. (e, f) Packing structure of **EtP6⊃G2**, showing an exo-wall tessellation host–guest complex.

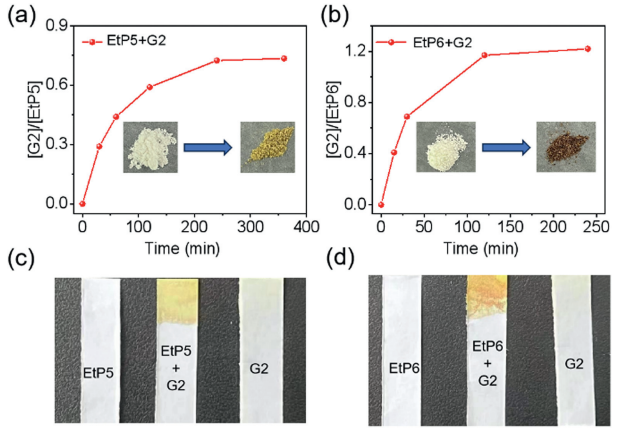

Fig. 6. (a) Time-dependent solid-liquid adsorption plot for **EtP5** towards **G2**. (b) Time-dependent solid-liquid adsorption plot for **EtP6** towards **G2**. The inserted photographs show the colour deepening of pillararenes upon the adsorption of guests. Test papers made from (c) **EtP5** and (d) **EtP6**, showing significant colour changes in detection of **G2**.

trifuged, washed with methanol and vacuum dried at room temperature. The adsorption efficiency was determined through the ^{1}H NMR spectra of these pillararenes (Figs. 6a and b, Figs. S14a and b, S15–S33 in Supporting information). For **G1**, Only **EtP6** was capable of effectively absorbing it from the solution (Figs. S14b, S20–S24 in Supporting information). **EtP5** shows no adsorption ability toward **G1** due to the weak host–guest interactions (Figs. S14a, S15–S19). For **G2**, we discovered that it can be efficiently removed by **EtP5** and **EtP6** from solution (Figs. 6a and b, Figs. S25–S33). Notably, **G2** is a highly hazardous compound known for its explosive and toxic properties, posing significant risks to human health and the environment. Therefore, the detection and removal of **G2** are of utmost importance. After adsorption at saturated point, the color of **EtP5** powder turned yellow upon absorbing **G2**, while that of **EtP6** powder turned brown (inset pictures in Figs. 6a and b). This change in color might be attributed to the intermolecular charge transfer interactions and may serve as an indicator for picric acid (**G2**) detection. Additionally, we prepared pillararene-based test papers by immersing the paper in a solution of pillararenes and allowing it to dry. The detection ability was indicated by the colour change of the test papers. Except for **EtP5** and **G1**, after adding several drops of guest solution to the test papers, a significant colour change occurred and could be easily visualized with the naked eye, which was distinctly different from the untreated paper (right one in Figs. 6c and d, Fig. S14d). The PXRD data of **EtP5**/**EtP6** before and after the adsorption of guest molecules were obtained (Fig. S34 in Supporting information). For **EtP5**/**EtP6**, the PXRD patterns of **EtP5**/**EtP6** were changed after adsorption of **G1**/**G2**. These results indicated the occurrence of structural transitions from guest-free **EtP5**/**EtP6** to a new **G1**/**G2**-loaded structure after adsorption of **G1**/**G2**.

In conclusion, our study focused on investigating the host–guest complexation behavior between perethylated pillar[*n*]arenes and two aromatic nitro guest molecules. The results from various techniques such as ^{1}H NMR, 2D NOESY NMR, and UV-vis spectroscopy, successfully confirmed the formation of stable complexes through host–guest interactions in solution. Additionally, the acquisition of three single crystal structures confirmed the formation of stable complexes in solid state, and further provided valuable insights into the diverse supramolecular arrangements observed in the solid state. These structures included a 1:1 host–guest inclusion complex for **EtP6** and **G1**, an external binding complex for **EtP5** and **G2**, and an exo-wall tessellation complex for **EtP6** and **G2**. Furthermore, our findings demonstrated the remarkable detection and adsorption capabilities of pillararenes towards these aromatic nitro compounds. Given the hazardous nature of these compounds, any potential leakage may possibly lead to severe consequences. Therefore, our results shed light on the potential for developing pillararene-based materials for the detection and adsorption of these compounds, thus providing great significance for environmental protection. Furthermore, the synthetic route for pillararenes is well-established and the yield is high, allowing for mass production at a relatively low cost, which holds potential for commercial viability. However, the selectivity of detection nitro compounds using this method relies significantly on the size and binding affinity of the macrocyclic host. A threshold for nitro compound adsorption by pillararenes also exists, leading to saturation beyond which no further adsorption occurs. Additionally, research on the biodegradability of pillararenes is limited. Future endeavors should focus on amplifying detection signals and designing porous structures capable of accommodating a greater variety of guests. Furthermore, incorporating macrocyclic hosts into biodegradable polymers represents a promising approach to enhance their biodegradability. Concurrently, we intend to investigate novel supramolecular macrocycles that are amenable to large-scale production, with the capability to detect a wider array of environmental contaminants. We are confident that ongoing innovation in this domain will significantly expand the effectiveness and applicability of adsorption and detection techniques, thereby making a substantial contribution to environmental remediation.

Declaration of competing interest

The authors declare that they have no known competing financial interests or personal relationships that could have appeared to influence the work reported in this paper.

CRediT authorship contribution statement

Xueru Zhao: Writing – review & editing, Writing – original draft, Validation, Software. **Aopu Wang:** Writing – review & editing, Writing – original draft, Validation. **Shimin Wang:** Writing – review & editing, Writing – original draft. **Zhijie Song:** Writing –

review & editing. **Li Ma:** Writing – review & editing. **Li Shao:** Writing – review & editing, Writing – original draft, Validation, Supervision, Methodology, Funding acquisition.

Acknowledgments

This work was supported by the fundamental research funds of Zhejiang Sci-Tech University (No. 22212286-Y) and the Natural Science Foundation of Zhejiang Province (No. LQ24B040003).

Supplementary materials

Supplementary material associated with this article can be found, in the online version, at doi:10.1016/j.cclet.2024.110205.

References

[1] F.Y. Zhong, C.Q. Li, Y.B. Xie, et al., J. Solid State Chem. 278 (2019) 120892.
[2] C.R. Qin, M.T. Dang, Y.F. Meng, et al., Process Saf. Environ. Prot. 172 (2023) 659–680.
[3] S. Roy, J. Darabdhara, M. Ahmaruzzaman, J. Clean. Prod. 430 (2023) 139517.
[4] M. Bastrakov, A. Starosotnikov, Pharmaceuticals 15 (2022) 705.
[5] Y.R. Jiang, X.F. Wang, M. Li, et al., J. Environ. Sci. 135 (2024) 483–494.
[6] Z.X. Fang, Y. Gu, X.R. Dong, et al., Chin. Chem. Lett. 34 (2023) 108128.
[7] M.Y. Liu, W.L. Zheng, Y. Yang, et al., Microchem. J. 191 (2023) 108889.
[8] Y.L. Hou, R.P. Shi, H.Y. Yuan, et al., Chin. Chem. Lett. 34 (2023) 107688.
[9] R.R. Nair, S. Debnath, R. Ghosh, et al., Chem. Eur. J. 30 (2023) e202303068.
[10] B. Jana, S. Ghorai, Y.R. Singh, et al., Mater. Today Chem. 33 (2023) 101684.
[11] M. Ueno, T. Tomita, H. Arakawa, et al., Commun. Chem. 3 (2020) 183.
[12] Q. Li, H.T.Z. Zhu, F.H. Huang, J. Am. Chem. Soc. 141 (2019) 13290–13294.
[13] Y. Jia, W.L. Guan, J. Liu, et al., Chin. Chem. Lett. 34 (2023) 108082.
[14] C.Y. Wang, Y.Q. Liu, C.G. Jia, et al., Chin. Chem. Lett. 34 (2023) 108400.
[15] X. Li, M.L. Shen, J. Yang, et al., Adv. Mater. 36 (2024) 2313317.
[16] E. Li, W.J. Zhu, S. Fang, et al., Angew. Chem. Int. Ed. 61 (2022) e202211780.
[17] K.C. Jie, Y.J. Zhou, Q. Sun, et al., Nat. Commun. 11 (2020) 1086.
[18] Z.D. Tang, X.M. Sun, T.T. Huang, et al., Chin. Chem. Lett. 34 (2023) 107698.
[19] P.B. Niu, C.H. Shi, J.M. Jiao, et al., Chem. Commun. 59 (2023) 10960–10963.
[20] S. Ohtani, K. Onishi, K. Wada, et al., Adv. Funct. Mater. 34 (2024) 2312304.
[21] T.X. Xiao, L. Zhou, X.Q. Sun, et al., Chin. Chem. Lett. 31 (2020) 1–9.
[22] L. Shao, H.W. Zhang, X.Q. He, et al., J. Am. Chem. Soc. 143 (2021) 693–698.
[23] B.B. Shi, J.X. Jiang, H. An, et al., J. Am. Chem. Soc. 146 (2024) 2901–2906.
[24] R.W. Tang, Y.P. Ye, S.J. Zhu, et al., Chin. Chem. Lett. 34 (2023) 107734.
[25] B. Hua, C. Zhang, W. Zhou, et al., J. Am. Chem. Soc. 142 (2020) 16557–16561.
[26] H.Z. Liang, Y.T. Yang, L. Shao, et al., J. Am. Chem. Soc. 145 (2023) 2870–2876.
[27] X.R. Zhao, B. Hua, L. Shao, Chem. Commun. 60 (2024) 1164–1167.
[28] M. Li, Y. Liu, L. Shao, et al., J. Am. Chem. Soc. 145 (2023) 667–675.